



HAL
open science

Accuracy of a Low Mach Number Model for Time-Harmonic Acoustics

Jean-François Mercier

► **To cite this version:**

Jean-François Mercier. Accuracy of a Low Mach Number Model for Time-Harmonic Acoustics. SIAM Journal on Applied Mathematics, 2018, 78 (4), pp.1891-1912. 10.1137/17M113976X . hal-04832135

HAL Id: hal-04832135

<https://hal.science/hal-04832135v1>

Submitted on 11 Dec 2024

HAL is a multi-disciplinary open access archive for the deposit and dissemination of scientific research documents, whether they are published or not. The documents may come from teaching and research institutions in France or abroad, or from public or private research centers.

L'archive ouverte pluridisciplinaire **HAL**, est destinée au dépôt et à la diffusion de documents scientifiques de niveau recherche, publiés ou non, émanant des établissements d'enseignement et de recherche français ou étrangers, des laboratoires publics ou privés.

41 Euler Equations, is to consider an intermediate between a potential flow and a general
 42 flow: a shear flow $\mathbf{v}_0 = u_0(y)\mathbf{e}_x$. Then the Linearized Euler Equations simplify in
 43 the Pridmore-Brown equation [7], which is a scalar ordinary differential equation.
 44 However, the numerical resolution of this equation is difficult [8], in particular due
 45 to the presence of a continuous spectrum of hydrodynamic modes and sometimes
 46 to the presence of unstable modes [9]. To solve this difficulty, a usual approach is
 47 to neglect hydrodynamic modes [8, 9, 10]. Another approach is to approximate a
 48 shear flow by a uniform flow. This is a natural approach for a boundary layer flow
 49 when the thickness of the layer is very small, but it is not always possible since
 50 such approximation can lead to ill-posed problems. It is in particular the case when
 51 studying the acoustic propagation in a duct with absorbing walls [11, 12]. In presence
 52 of a uniform flow, these walls are classically described by the Myers condition [13],
 53 but this condition leads to several theoretical and numerical troubles [14]. On the
 54 contrary, the problem is well-posed in presence of a shear flow vanishing on the wall,
 55 because the Myers condition becomes a simple Robin condition. But the shear flow
 56 introduces hydrodynamic modes. To recover the comfort of dealing with a uniform
 57 flow, improved Myers conditions have been derived [15], allowing to consider a uniform
 58 flow while leading to a well-posed problem.

59 In this paper we propose to go beyond the restrictions to a uniform, a shear or
 60 a potential flow and to go toward a more general flow while keeping a simple model.
 61 To deal with a general flow, different wave-like models are available, among which
 62 the Galbrun equation [16, 17, 18], the Möhring equations [19, 20] and the Goldstein's
 63 equations [21, 22, 23, 24]. We choose the Goldstein equations (4)-(5), linking two
 64 unknowns, the velocity potential φ and the hydrodynamic vector field $\boldsymbol{\xi}$, because: (i)
 65 they are a direct extension of the potential wave equation (1), (ii) they are simpler than
 66 alternative models: in the area where the carrier flow is potential, it can be proved
 67 that $\boldsymbol{\xi}$ vanishes and the Goldstein equations degenerate in the convected Helmholtz
 68 equation (1), (iii) the unknowns of Goldstein's equations have a physical meaning: φ
 69 represents the acoustical field whereas $\boldsymbol{\xi}$ describes the hydrodynamic phenomena.

70 An interesting application of Goldstein equations is to give the possibility to relate
 71 a hydrodynamic field and an acoustic field when studying the gust-aerofoil interaction
 72 noise. It has been done for potential [25] and for tranverse shear flows [26, 27]. The
 73 derived theoretical models are precise but rather complex, involving integration in
 74 the complex plane in presence of poles and branch cuts, Wiener-Hopf techniques or
 75 asymptotic expansions. Simplifications are obtained by restricting to the far-field
 76 behavior or to low frequencies. In this paper we will rather focus on building a model
 77 both very simple and valid at all frequencies and for the near-field and the far-field,
 78 but that will be justified only for flows of moderate speed.

79 The aim of this paper is the following: to propose an aeroacoustic model, defined
 80 for a general flow, simpler than the general Goldstein equations, but still taking into
 81 account hydrodynamic effects. Starting from the Goldstein equations, we will derive
 82 a simpler model, called the Low Mach number model Eq. (10). This model will be
 83 designed to be very well adapted to slow flows and we postulate that it is a good
 84 approximation for non-slow flows. Restricting to a 1D shear flow (Eq. (11)) for the
 85 theory, by deriving precise estimates we will prove that the corresponding Low Mach
 86 number model Eq. (12) remains of good quality for moderate velocity flows.

87 The paper is organized as follows. In the second section are given the Goldstein
 88 equations, for a general flow and simplified expressions for two classes of flows: a
 89 slow flow and a parallel shear flow. The rest of the paper focuses on estimating
 90 theoretically the quality of the Low Mach number model. It will be done in the case

91 of a shear flow, leading to a complete theory. In section 3, introducing a dissipative
 92 problem to simplify the treatment of radiation conditions, the Goldstein equations
 93 are proved to be well-posed. The simplifications induced when considering a slow
 94 flow and the link with the no-flow problem are presented in section 4. The alternative
 95 model to the Goldstein equations, the Low Mach number model Eq. (12), is precisely
 96 characterized in section 5 and the quality of this approximation is quantified. Finally,
 97 the theoretical estimates are validated numerically in section 6.

98 **2. Equations of the problem.**

99 **2.1. Goldstein’s equations for a general flow.** The flow is taken stationary
 100 and homentropic (entropy is constant and uniform). It is characterized by its non
 101 uniform fields of velocity \mathbf{v}_0 , density ρ_0 , pressure p_0 and solves the stationary Euler
 102 Equations:

$$103 \quad (3) \quad \begin{cases} \nabla \cdot (\rho_0 \mathbf{v}_0) = 0, \\ \rho_0 (\mathbf{v}_0 \cdot \nabla) \mathbf{v}_0 + \nabla p_0 = 0, \\ p_0 = \mu \rho_0^\gamma, \end{cases}$$

104 where ρ_0 is the density p_0 is the pressure. The state law reduces to a barotropic law
 105 (the pressure depends only on the density) for an homentropic flow. The physical
 106 constants γ and μ characterize this state law. On rigid boundaries we have $\mathbf{v}_0 \cdot \mathbf{n} = 0$.

107 For the acoustic perturbations, the velocity potential φ and $\boldsymbol{\xi}$, the hydrodynamic
 108 unknown, satisfy the Goldstein equations:

$$109 \quad (4) \quad D_\omega \left(\frac{1}{c_0^2} D_\omega \varphi \right) = \frac{1}{\rho_0} \nabla \cdot [\rho_0 (\nabla \varphi + \boldsymbol{\xi})],$$

$$110 \quad (5) \quad D_\omega \boldsymbol{\xi} = \nabla \varphi \times \boldsymbol{\omega}_0 - (\boldsymbol{\xi} \cdot \nabla) \mathbf{v}_0.$$

111 with

$$112 \quad (6) \quad \boldsymbol{\omega}_0 = \nabla \times \mathbf{v}_0,$$

113 the vorticity of the carrier flow. The sound speed c_0 is given by

$$114 \quad (7) \quad c_0^2 = \gamma \frac{p_0}{\rho_0}.$$

115 The velocity and pressure are deduced thanks to [21]

$$116 \quad \begin{cases} \mathbf{v} = \nabla \varphi + \boldsymbol{\xi}, \\ p = -\rho_0 D_\omega \varphi. \end{cases}$$

117 In presence of rigid boundaries, the unknowns satisfy

$$118 \quad \mathbf{v} \cdot \mathbf{n} = \frac{\partial \varphi}{\partial n} + \boldsymbol{\xi} \cdot \mathbf{n} = 0.$$

119 As mentioned in the introduction, we will not solve the Goldstein equations in the
 120 general case. Now we present two configurations, for which the Goldstein equations
 121 simplify: a 2D slow flow and a parallel shear flow.

122 **2.2. Goldstein's equations for a slow flow.** The Goldstein equations (4)-(5)
 123 in the general case are complicated to solve, on a theoretical and a numerical point
 124 of view. Eq. (4) is rather classic: for a fixed value of ξ , $\nabla \cdot \xi$ in (4) can be considered
 125 as a source term and φ satisfies the classical convected Helmholtz equation (1), in
 126 particular associated to classical radiation conditions. A consequence is that it can be
 127 solved numerically, using continuous finite elements and classical Perfectly Matched
 128 Layers (PMLs) to bound the calculation domain [28, 29, 30]. On the contrary, for
 129 a fixed value of φ , ξ in (5) satisfies an harmonic transport equation. This equation
 130 is classical in the time domain (solved by the characteristics method) but not in the
 131 harmonic domain. In particular, this equation is difficult to solve numerically: the use
 132 of Lagrange finite elements to approximate this transport equation leads to polluted
 133 results and it has to be solved with other methods like with discontinuous finite
 134 elements [31, 32]. Also the radiation conditions are replaced by a causality condition
 135 [18]. A consequence is that the introduction of PMLs is not straightforward.

136 Let us write the harmonic transport equation (5) in the form $L\xi = \nabla\varphi \times \omega_0$,
 137 where

$$138 \quad (8) \quad L\xi = -i\omega\xi + (\mathbf{v}_0 \cdot \nabla)\xi + (\xi \cdot \nabla)\mathbf{v}_0.$$

139 The difficulty is to determine L^{-1} . In general, its determination requires to integrate
 140 the transport equation along the streamlines of the flow. This procedure will be
 141 presented later in the case of a parallel-shear flow, leading to explicit expressions.
 142 But in general, this has to be done numerically.

143 To express the hydrodynamic unknown versus the velocity potential in a simple
 144 way, a first approximation is to take $\xi = \mathbf{0}$ (then Eq. (1) is recovered). This ap-
 145 proximation is exact only for a uniform flow or for a potential flow, but for a vortical
 146 flow, it is in general inaccurate. The situation is much simpler if the flow is slow,
 147 in the sense \mathbf{v}_0 and $|\nabla\mathbf{v}_0|$ are small. Then ξ can be obtained explicitly versus φ :
 148 the operator L can be replaced by $-i\omega$ and the hydrodynamic unknown is obtained
 149 explicitly versus the velocity potential

$$150 \quad (9) \quad \xi = i(\nabla\varphi \times \omega_0)/\omega.$$

151 This leads to the Low Mach number model:

$$152 \quad (10) \quad D_\omega \left(\frac{1}{c_0^2} D_\omega \varphi \right) = \frac{1}{\rho_0} \nabla \cdot \left[\rho_0 \left(\nabla\varphi + \frac{i}{\omega} (\nabla\varphi \times \omega_0) \right) \right].$$

153 The idea of simplifying an aeroacoustic problem by restricting to a low Mach number
 154 flow has been also introduced for a potential flow [1, 33, 34], shear flows [35], Gal-
 155 brun's equation [36] or Linearised Euler's Equations [37, 38]. However in all these
 156 cases, no error estimates have been derived. On the contrary, in this paper and for
 157 a shear flow we will quantify the error committed when using the Low Mach number
 158 approximation. We will show the main result of this paper: this approximation is
 159 very good, of order two in the sense that the error on φ is bounded by the square of
 160 the Mach number $M = \sup_{\mathbf{x} \in \Omega} |\mathbf{v}_0|/c_0$.

161 **REMARK 1.** *Note that, since the assumption \mathbf{v}_0 and $|\nabla\mathbf{v}_0|$ small implies that $|\omega_0|$
 162 is small, the Low Mach number approximation seems to indicate that $\xi = \mathbf{0}$ is a good
 163 approximation. However, we will prove that it is a crude first order approximation
 164 since it leads to an error bounded only by M , not M^2 .*

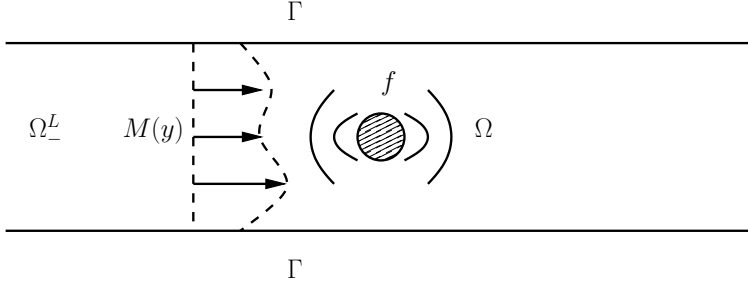


FIG. 1. Acoustic source radiating in a shear flow in an infinite duct

165 **REMARK 2.** Note that (9) has the advantage to be a closed form formula but it
 166 leads to ξ less regular than φ since it differentiates φ . On the contrary, L in Eq. (8)
 167 does not give ξ explicitly but is a zero order operator in the sense that ξ and φ have
 168 the same regularity (this will be proved in the shear flow case).

169 **2.3. Case of a shear flow in a duct.** To simplify the presentation of the
 170 Low Mach number approximation, we will consider a 2D rectangular geometry $\Omega =$
 171 $\mathbb{R} \times (0, h)$ with the cartesian coordinates (x, y) and we will consider a parallel shear
 172 flow $\mathbf{v}_0 = v_0(y)\mathbf{e}_x$ with $v_0 \in C^1([0, h])$. Then from (6) we get $\boldsymbol{\omega}_0 = -v_0'\mathbf{e}_z$ where
 173 $\mathbf{e}_z = \mathbf{e}_x \times \mathbf{e}_y$, from Euler's equations (3) we get $\rho_0 = \text{cst}$, $p_0 = \text{cst}$ and from Eq.
 174 (7) is deduced $c_0 = \text{cst}$. For such shear flow, introducing the Mach number profile
 175 $M(y) = v_0(y)/c_0$, $M'(y) = dM/dy$ and noting $D = M(y)\partial/\partial x - ik$ with $k = \omega/c_0$,
 176 the Goldstein equations take the simpler form:

$$177 \quad (11) \quad \left\{ \begin{array}{l} D^2\varphi = \nabla \cdot (\nabla\varphi + \boldsymbol{\xi}) + f \quad \text{in } \Omega, \\ D\boldsymbol{\xi} = \begin{pmatrix} -M' \left(\frac{\partial\varphi}{\partial y} + \xi_y \right) \\ M' \frac{\partial\varphi}{\partial x} \end{pmatrix} \quad \text{in } \Omega, \\ \frac{\partial\varphi}{\partial y} + \xi_y = 0 \quad \text{on } \partial\Omega, \end{array} \right.$$

178 where $\partial\Omega = \{(x, y)/y = 0 \text{ or } y = h\}$, $\boldsymbol{\xi} = (\xi_x, \xi_y)^T$ and where we have introduced a
 179 source term $f \in L^2(\Omega)$ to consider a radiation problem (see Fig. 1). The Low Mach
 180 number approximation (9) written for a shear flow consists in taking

$$181 \quad \left\{ \begin{array}{l} \xi_x = -\frac{iM'(y)}{k} \frac{\partial\varphi}{\partial y}, \\ \xi_y = \frac{iM'(y)}{k} \frac{\partial\varphi}{\partial x}, \end{array} \right.$$

182 and leads to the Low Mach number model for a shear flow:

$$183 \quad (12) \quad \left\{ \begin{array}{l} D^2\varphi - \Delta\varphi = \frac{i}{k} \left[\frac{\partial}{\partial y} \left(M'(y) \frac{\partial\varphi}{\partial x} \right) - \frac{\partial}{\partial x} \left(M'(y) \frac{\partial\varphi}{\partial y} \right) \right] + f \quad \text{in } \Omega, \\ \frac{\partial\varphi}{\partial y} + \frac{iM'(y)}{k} \frac{\partial\varphi}{\partial x} = 0 \quad \text{on } \partial\Omega. \end{array} \right.$$

184 To close this radiation problem and to prove its well-posedness, we need to intro-
185 duce some radiation conditions, which is done in the next section.

186 **3. Well-posedness of the dissipative problem in an infinite duct.** In this
187 part, we introduce the dissipative problem to simplify the description of the radiation
188 conditions of problem (11). Then we prove that the dissipative problem is well-posed
189 under the condition of a subsonic flow.

190 **3.1. The dissipative problem.** We consider the dissipative problem where the
191 wave number is extended to the complex plane:

$$192 \quad k_\varepsilon = k + i\varepsilon, \quad \varepsilon > 0.$$

193 Thanks to the dissipation ε , the outgoing solution corresponds to the solution with
194 a finite energy (which stands for the radiation condition): the velocity potential is
195 sought in $H^1(\Omega)$ and $\boldsymbol{\xi}$ is sought in $(L^2(\Omega))^2$, which leads to $\boldsymbol{v} = \nabla\varphi + \boldsymbol{\xi}$ in $(L^2(\Omega))^2$.
196 To simplify our study, we suppose that the flow does not vanish:

$$197 \quad M(y) > 0 \quad \forall y \in [0, h].$$

198 Let us consider the following problem, which is problem (11) with k replaced by k_ε :
199 find $\varphi \in H^1(\Omega)$ and $\boldsymbol{\xi} \in (L^2(\Omega))^2$ such that

$$200 \quad (13) \quad \left\{ \begin{array}{ll} D_\varepsilon^2 \varphi = \nabla \cdot (\nabla \varphi + \boldsymbol{\xi}) + f & \text{in } \Omega, \\ D_\varepsilon \boldsymbol{\xi} = \begin{pmatrix} -M' \left(\frac{\partial \varphi}{\partial y} + \xi_y \right) \\ M' \frac{\partial \varphi}{\partial x} \end{pmatrix} & \text{in } \Omega, \\ \frac{\partial \varphi}{\partial y} + \xi_y = 0 & \text{on } \partial\Omega, \end{array} \right.$$

201 where

$$202 \quad D_\varepsilon = M(y) \frac{\partial}{\partial x} - ik_\varepsilon.$$

203 The strategy to prove the well-posedness of Eq. (13) is to decouple the treatments
204 of the acoustics and the hydrodynamic phenomena and is the following:

- 205 • first we solve the hydrodynamic equation of (13). The solution is noted
- 206 $\boldsymbol{\xi} = \mathbf{A}_\varepsilon \varphi$ and we prove that \mathbf{A}_ε is continuous from $H^1(\Omega)$ onto $(L^2(\Omega))^2$.
- 207 • second we solve the acoustic part of (13):

$$208 \quad \left\{ \begin{array}{ll} D_\varepsilon^2 \varphi - \nabla \cdot (\nabla \varphi + \mathbf{A}_\varepsilon \varphi) = f & \text{in } \Omega, \\ \frac{\partial \varphi}{\partial y} + A_\varepsilon^y \varphi = 0 & \text{on } \partial\Omega. \end{array} \right.$$

209 **3.2. The hydrodynamic equation.**

210 **THEOREM 1.** *The second equation of (13) admits a unique solution in $(L^2(\Omega))^2$:*

$$211 \quad \boldsymbol{\xi} = \mathbf{A}_\varepsilon \varphi = [(A_\varepsilon^{x,1} + A_\varepsilon^{x,2})\varphi, A_\varepsilon^y \varphi]^T,$$

212 where

$$\begin{cases}
 A_\varepsilon^{x,1}\varphi &= -\frac{M'(y)}{M(y)} \int_{-\infty}^x e^{i\frac{k_\varepsilon}{M(y)}(x-s)} \frac{\partial\varphi}{\partial y}(s, y) ds, \\
 A_\varepsilon^{x,2}\varphi &= -\left(\frac{M'(y)}{M(y)}\right) \int_{-\infty}^x (x-s) e^{i\frac{k_\varepsilon}{M(y)}(x-s)} \frac{\partial\varphi}{\partial x}(s, y) ds, \\
 A_\varepsilon^y\varphi &= \frac{M'(y)}{M(y)} \int_{-\infty}^x e^{i\frac{k_\varepsilon}{M(y)}(x-s)} \frac{\partial\varphi}{\partial x}(s, y) ds.
 \end{cases}
 \tag{14}$$

Moreover \mathbf{A}_ε is continuous from $H^1(\Omega)$ onto $(L^2(\Omega))^2$ with the inequality

$$\|\mathbf{A}_\varepsilon\varphi\|_{L^2(\Omega)^2} \leq \sqrt{2} \frac{S_1}{\varepsilon} \left(1 + \frac{S_1}{\varepsilon}\right) \|\nabla\varphi\|_{L^2(\Omega)^2},
 \tag{15}$$

where $S_1 = \max_{y \in [0, h]} |M'(y)|$.

Proof. By linearity, $\boldsymbol{\xi}$ may be sought in the form

$$\boldsymbol{\xi} = (\xi_x^1 + \xi_x^2, \xi_y)^T,$$

where

$$\begin{cases}
 D_\varepsilon \xi_x^1 &= -M' \frac{\partial\varphi}{\partial y}, \\
 D_\varepsilon \xi_x^2 &= -M' \xi_y, \\
 D_\varepsilon \xi_y &= M' \frac{\partial\varphi}{\partial x}.
 \end{cases}
 \tag{16}$$

The second equation for ξ_x^2 implies that $D_\varepsilon^2 \xi_x^2 = -M'^2 \frac{\partial\varphi}{\partial x}$.

The uniqueness in $L^2(\Omega)$ is straightforward since the solutions of the homogeneous equation $D_\varepsilon \zeta = 0$, which are $a(y)e^{ik_\varepsilon x/M(y)}$, cannot belong to $L^2(\Omega)$, except if $a = 0$.

Then it is easy to check that the causal Green functions:

$$\begin{aligned}
 G_\varepsilon(x, y) &= \frac{Y(x)}{M(y)} e^{i\frac{k_\varepsilon}{M(y)}x}, \\
 \tilde{G}_\varepsilon(x, y) &= \frac{Y(x)}{M(y)^2} x e^{i\frac{k_\varepsilon}{M(y)}x},
 \end{aligned}$$

with Y the Heaviside function, are the unique functions $\in L^2(\Omega)$ satisfying for every $y \in [0, h]$:

$$\begin{aligned}
 D_\varepsilon G_\varepsilon(x, y) &= \delta(x), \\
 D_\varepsilon^2 \tilde{G}_\varepsilon(x, y) &= \delta(x).
 \end{aligned}$$

The expression of $\boldsymbol{\xi}$ is finally obtained by convolution of the right hand sides in (16) with G_ε and \tilde{G}_ε :

$$\begin{cases}
 \xi_x^1 = A_\varepsilon^{x,1}\varphi &= G_\varepsilon * \left(-M' \frac{\partial\varphi}{\partial y}\right), \\
 \xi_x^2 = A_\varepsilon^{x,2}\varphi &= \tilde{G}_\varepsilon * \left(-M'^2 \frac{\partial\varphi}{\partial x}\right), \\
 \xi_y = A_\varepsilon^y\varphi &= G_\varepsilon * M' \frac{\partial\varphi}{\partial x}.
 \end{cases}$$

234 Finally, to prove that ξ is in $(L^2(\Omega))^2$, let us recall that a direct application of Cauchy-
 235 Schwartz inequality leads to: if $h \in L^2(\mathbb{R})$ and $g \in L^1(\mathbb{R})$, then $h * g \in L^2(\mathbb{R})$ and

$$236 \quad \|h * g\|_{L^2(\mathbb{R})} \leq \|h\|_{L^2(\mathbb{R})} \|g\|_{L^1(\mathbb{R})}. \quad \square$$

237 Since a simple calculation gives $\|G_\varepsilon\|_{L^1(\mathbb{R})} = 1/\varepsilon$ and $\|\tilde{G}_\varepsilon\|_{L^1(\mathbb{R})} = 1/\varepsilon^2$, we get
 238 finally:

$$\begin{aligned} 239 \quad \|\mathbf{A}_\varepsilon \varphi\|_{L^2(\mathbb{R})^2}^2 &= \int_{\mathbb{R}} \left(|(A_\varepsilon^{x,1} + A_\varepsilon^{x,2})\varphi|^2 + |A_\varepsilon^y \varphi|^2 \right) dx, \\ 240 \quad &\leq 2 \int_{\mathbb{R}} \left(|A_\varepsilon^{x,1} \varphi|^2 + |A_\varepsilon^{x,2} \varphi|^2 + |A_\varepsilon^y \varphi|^2 \right) dx, \\ 241 \quad &\leq 2 \left[\frac{|M'|^2}{\varepsilon^2} \int_{\mathbb{R}} \left| \frac{\partial \varphi}{\partial y} \right|^2 dx + \frac{|M'|^4}{\varepsilon^4} \int_{\mathbb{R}} \left| \frac{\partial \varphi}{\partial x} \right|^2 dx + \frac{|M'|^2}{\varepsilon^2} \int_{\mathbb{R}} \left| \frac{\partial \varphi}{\partial x} \right|^2 dx \right], \\ 242 \quad &\leq 2 \frac{S_1^2}{\varepsilon^2} \left(1 + \frac{S_1^2}{\varepsilon^2} \right) \int_{\mathbb{R}} |\nabla \varphi|^2 dx. \end{aligned}$$

243 Integration on $y \in]0, h[$ gives the constant in (15).

244 **3.3. Variational formulation.** By injecting the expression of ξ in the first
 245 equation of (13), the following problem of unknown φ is obtained: find $\varphi \in H^1(\Omega)$
 246 such that

$$247 \quad \begin{cases} D_\varepsilon^2 \varphi - \nabla \cdot (\nabla \varphi + \mathbf{A}_\varepsilon \varphi) = f & \text{in } \Omega, \\ \frac{\partial \varphi}{\partial y} + A_\varepsilon^y \varphi = 0 & \text{on } \partial\Omega. \end{cases}$$

248 This problem has good mathematical properties: for instance, the Lax-Milgram
 249 theorem applies if ε is large enough. To prove this, let us first derive the variational
 250 formulation of the problem:

$$251 \quad (17) \quad \begin{cases} \text{Find } \varphi \in H^1(\Omega) \text{ such that } \forall \psi \in H^1(\Omega), \\ a_\varepsilon(\varphi, \psi) = \int_{\Omega} f \bar{\psi}, \end{cases}$$

252 where $a_\varepsilon(\varphi, \psi) = b_\varepsilon(\varphi, \psi) + c_\varepsilon(\varphi, \psi)$ with

$$\begin{aligned} 253 \quad b_\varepsilon(\varphi, \psi) &= \int_{\Omega} (1 - M^2) \frac{\partial \varphi}{\partial x} \frac{\partial \bar{\psi}}{\partial x} + \frac{\partial \varphi}{\partial y} \frac{\partial \bar{\psi}}{\partial y} - 2ik_\varepsilon M \frac{\partial \varphi}{\partial x} \bar{\psi} - k_\varepsilon^2 \varphi \bar{\psi}, \\ 254 \quad c_\varepsilon(\varphi, \psi) &= \int_{\Omega} (\mathbf{A}_\varepsilon \varphi) \cdot \nabla \bar{\psi}. \end{aligned}$$

255 **THEOREM 2.** *The variational problem (17) is well-posed for $S_0 = \max_{y \in [0, h]} |M(y)| < \blacksquare$*
 256 *1 and ε large enough.*

257 *Proof.* We just need to prove that the sesquilinear form $a_\varepsilon(\varphi, \psi)$ is coercive. Con-
 258 cerning the sesquilinear form $b_\varepsilon(\varphi, \psi)$, first we note that

$$259 \quad |b_\varepsilon(\varphi, \varphi)| = \left| \frac{k_\varepsilon}{k_\varepsilon} b_\varepsilon(\varphi, \varphi) \right| \geq |k_\varepsilon| \Im m \left(-\frac{b_\varepsilon(\varphi, \varphi)}{k_\varepsilon} \right).$$

260 An integration by parts for all φ in $H^1(\Omega)$ leading to

$$261 \quad \int_{\Omega} \frac{\partial \varphi}{\partial x} \bar{\varphi} \in i\mathbb{R},$$

262 we get

$$\begin{aligned} 263 \quad \Im m \left(-\frac{b_{\varepsilon}(\varphi, \varphi)}{k_{\varepsilon}} \right) &= \int_{\Omega} \frac{\varepsilon}{|k_{\varepsilon}|^2} \left[(1 - M^2) \left| \frac{\partial \varphi}{\partial x} \right|^2 + \left| \frac{\partial \varphi}{\partial y} \right|^2 \right] + \varepsilon |\varphi|^2, \\ 264 \quad &\geq \frac{\varepsilon}{|k_{\varepsilon}|^2} (1 - S_0^2) \|\nabla \varphi\|_{L^2(\Omega)^2}^2 + \varepsilon \|\varphi\|_{L^2(\Omega)}^2, \\ 265 \quad &\geq \min \left(\frac{\varepsilon}{|k_{\varepsilon}|^2} (1 - S_0^2), \varepsilon \right) \|\varphi\|_{H^1(\Omega)}^2. \end{aligned}$$

266 Concerning the sesquilinear form $c_{\varepsilon}(\varphi, \psi)$, we get thanks to Theorem 1:

$$267 \quad |c_{\varepsilon}(\varphi, \varphi)| \leq \|\mathbf{A}_{\varepsilon} \varphi\|_{L^2(\Omega)^2} \|\nabla \varphi\|_{L^2(\Omega)^2} \leq \sqrt{2} \frac{S_1}{\varepsilon} \left(1 + \frac{S_1}{\varepsilon} \right) \|\nabla \varphi\|_{L^2(\Omega)^2}^2.$$

268 Combining the two previous results we get

$$269 \quad (18) \quad |a_{\varepsilon}(\varphi, \varphi)| \geq C_{\varepsilon}^c \|\varphi\|_{H^1(\Omega)}^2,$$

270 with

$$271 \quad (19) \quad C_{\varepsilon}^c = \min \left(\left[\frac{\varepsilon}{|k_{\varepsilon}|} (1 - S_0^2) - \sqrt{2} \frac{S_1}{\varepsilon} \left(1 + \frac{S_1}{\varepsilon} \right) \right], \varepsilon |k_{\varepsilon}| \right).$$

272 Since

$$273 \quad \lim_{\varepsilon \rightarrow \infty} C_{\varepsilon}^c = 1 - S_0^2 > 0,$$

274 C_{ε}^c is positive for ε large enough. □

275 **REMARK 3.**

- 276 • to get well-posedness, the flow must be subsonic: $S_0 < 1$,
- 277 • for a uniform flow, $S_1 = 0$ and the problem is well-posed for all ε values.
- 278 $S_1 > 0$ means that we are in presence of a shear flow which may produce
- 279 instabilities [39]: then enough dissipation ε must be introduced to absorb the
- 280 energy of the instabilities.

281 **4. The restriction to a slow flow.** In the rest of the paper, we consider the
 282 dissipative problem for a slow shear flow, presented in the previous section. We
 283 consider a particular family of flows of the general form

$$284 \quad (20) \quad M(y) = Mm(y),$$

285 with M a constant such that $0 \leq M < 1$ and $m(y)$ a strictly positive fixed $C^2([0, h])$
 286 function with $\max_{y \in [0, h]} |m(y)| = 1$. Contrary to the previous section, we suppose
 287 that the dissipation ε is fixed and M is the only variable parameter. We note \mathbf{A}_M
 288 instead of \mathbf{A}_{ε} defined in Eq. (14) the hydrodynamic operator and φ_M the solution
 289 of Goldstein's equations (17). First we will prove that the solution φ_M exists for
 290 M small enough. Then we will show that the no flow solution φ_0 , although easy to
 291 determine (then $\mathbf{A}_M = \mathbf{A}_0 = \mathbf{0}$), is not a good approximation of φ_M . Indeed we will
 292 prove that the error $\|\varphi_M - \varphi_0\|_{H^1(\Omega)}$ is only of order M .

293 **4.1. Existence and unicity of the exact solution.** Let us prove first that,
 294 for any ε values, the problem (17) is well-posed for M small enough (previously we
 295 have proved that this problem is well-posed for M fixed and ε large enough). This
 296 problem is now written

$$297 \quad (21) \quad \begin{cases} \text{Find } \varphi \in H^1(\Omega) \text{ such that } \forall \psi \in H^1(\Omega), \\ a_M(\varphi, \psi) = \int_{\Omega} f \bar{\psi}, \end{cases}$$

298 where $a_M(\varphi, \psi) = a_0(\varphi, \psi) + b_M(\varphi, \psi) + c_M(\varphi, \psi)$ with

$$299 \quad (22) \quad a_0(\varphi, \psi) = \int_{\Omega} \nabla \varphi \cdot \nabla \bar{\psi} - k_{\varepsilon}^2 \varphi \bar{\psi},$$

$$300 \quad (23) \quad b_M(\varphi, \psi) = \int_{\Omega} -M^2 m(y)^2 \frac{\partial \varphi}{\partial x} \frac{\partial \bar{\psi}}{\partial x} - 2ik_{\varepsilon} M m(y) \frac{\partial \varphi}{\partial x} \bar{\psi},$$

$$301 \quad (24) \quad c_M(\varphi, \psi) = \int_{\Omega} (\mathbf{A}_M \varphi) \cdot \nabla \bar{\psi}.$$

302 **THEOREM 3.** *The variational problem (21) is well-posed for M small enough and*
 303 *its solution φ_M satisfies*

$$304 \quad (25) \quad C_M^c \|\varphi_M\|_{H^1(\Omega)} \leq \|f\|_{L^2(\Omega)},$$

305 where

$$306 \quad (26) \quad C_M^c = \min \left(\left[\frac{\varepsilon}{|k_{\varepsilon}|} (1 - M^2 s_0^2) - \sqrt{2} \frac{M s_1}{\varepsilon} \left(1 + \frac{M s_1}{\varepsilon} \right) \right], \varepsilon |k_{\varepsilon}| \right),$$

307 with $s_0 = \max_{y \in [0, h]} |m(y)|$ and $s_1 = \max_{y \in [0, h]} |m'(y)|$.

308 *Proof.* Following the proof of Theorem 2, using Eq. (15) we have

$$309 \quad (27) \quad \|\mathbf{A}_M \varphi\|_{L^2(\Omega)^2} \leq \sqrt{2} \frac{M s_1}{\varepsilon} \left(1 + \frac{M s_1}{\varepsilon} \right) \|\nabla \varphi\|_{L^2(\Omega)^2},$$

310 and the problem (21) is well-posed if $C_M^c > 0$ (C_M^c is C_{ε}^c in Eq. (19)). To conclude,
 311 we just notice that for M small enough

$$312 \quad C_M^c \sim C_0^c = \min \left(\frac{\varepsilon}{|k_{\varepsilon}|}, \varepsilon |k_{\varepsilon}| \right) > 0.$$

313 To prove that φ_M is bounded in $H^1(\Omega)$, we determine a lower bound and an
 314 upper bound of $|a_M(\varphi_M, \varphi_M)|$. The lower bound is deduced from the coercivity of
 315 $a_M(\varphi, \varphi)$ with the constant C_M^c (see Eq. (18)). For the upper bound, from (21) we
 316 get

$$317 \quad |a_M(\varphi_M, \psi)| \leq \|f\|_{L^2(\Omega)} \|\psi\|_{H^1(\Omega)}.$$

318 Taking $\psi = \varphi_M$ leads to (25). □

319 **4.2. Convergence to the no flow case.** In this part we first show that $\varphi_M \rightarrow$
 320 φ_0 when $M \rightarrow 0$ where φ_0 is the solution of the problem without flow and also that
 321 φ_0 approximates φ_M at the order M .

322 **4.2.1. The no flow model.** With no flow, $\varphi_M = \varphi_0$ is the solution of:

$$323 \quad (28) \quad \begin{cases} \text{Find } \varphi \in H^1(\Omega) \text{ such that } \forall \psi \in H^1(\Omega), \\ a_0(\varphi, \psi) = \int_{\Omega} f \bar{\psi}, \end{cases}$$

324 where $a_0(\varphi, \psi)$ is defined in Eq. (22). The sesquilinear form a_0 coincides with a_M for
 325 $M = 0$ and therefore the problem (28) is well posed with the coercivity constant C_0^c
 326 defined in (26), taking $M = 0$. In the following, to establish (32) we will need more
 327 regularity for φ_0 and we have the

328 LEMMA 4. *The solution φ_0 of (28) belongs to $H^2(\Omega)$.*

329 *Proof.* This is due to the regularity result [40, Theorem IX.26 page 182]:

$$330 \quad \{\varphi \in H^1(\Omega), \Delta\varphi \in L^2(\Omega), \partial\varphi/\partial y = 0 \text{ on } \partial\Omega\} = H^2(\Omega). \quad \square$$

331 **4.2.2. Quality of the no flow approximation.** We show now that φ_0 approx-
 332 imates φ_M at the order M :

333 THEOREM 5. *Let φ_0 and φ_M be the solution of (21) and (28). For M small*
 334 *enough, we have*

$$335 \quad \|\varphi_M - \varphi_0\|_{H^1(\Omega)} \leq M \frac{C_0}{C_0^c C_M^c} \|f\|_{L^2(\Omega)},$$

336 where C_M^c and C_0^c are defined in (26) and where

$$337 \quad (29) \quad C_0 = s_0^2 + 2|k_\varepsilon|s_0 + \sqrt{2} \frac{s_1}{\varepsilon} \left(1 + \frac{s_1}{\varepsilon}\right),$$

338 with $s_0 = \max_{y \in [0, h]} |m(y)|$ and $s_1 = \max_{y \in [0, h]} |m'(y)|$.

339 REMARK 4. *M small enough simply means that M is such that $C_M^c > 0$. Note*
 340 *also that for M small, C_M^c may be approximated by C_0^c which implies that $\|\varphi_M -$
 341 $\varphi_0\|_{H^1(\Omega)}$ is then bounded exactly by M (not M^n with $n < 1$).*

342 *Proof.* The solution φ_M satisfies (21) with

$$343 \quad a_M(\varphi_M, \psi) = a_0(\varphi_M, \psi) + d_M(\varphi_M, \psi),$$

344 where we have introduced

$$345 \quad d_M(\varphi, \psi) = b_M(\varphi, \psi) + c_M(\varphi, \psi) =$$

$$346 \quad - \left(\int_{\Omega} M^2 m(y)^2 \frac{\partial \varphi_M}{\partial x} \frac{\partial \bar{\psi}}{\partial x} + 2ik_\varepsilon M m(y) \frac{\partial \varphi_M}{\partial x} \bar{\psi} \right) + \int_{\Omega} (\mathbf{A}_M \varphi_M) \cdot \nabla \bar{\psi},$$

348 with b_M and c_M defined in (23) and (24). To evaluate $\|\varphi_M - \varphi_0\|_{H^1(\Omega)}$, we will
 349 establish the following inequality:

$$350 \quad (30) \quad \begin{cases} C_0^c \|\varphi_M - \varphi_0\|_{H^1(\Omega)}^2 & \leq |a_0(\varphi_M - \varphi_0, \varphi_M - \varphi_0)|, \\ & \leq MC_0 \|\varphi_M\|_{H^1(\Omega)} \|\varphi_M - \varphi_0\|_{H^1(\Omega)}. \end{cases}$$

351 The left hand side is simply due to the coercivity of the problem without flow.
 352 To get the right hand side, we start from the following relations $\forall \psi \in H^1(\Omega)$:

$$353 \quad \begin{cases} a_0(\varphi_M, \psi) + d_M(\varphi_M, \psi) &= \int_{\Omega} f \bar{\psi}, \\ a_0(\varphi_0, \psi) &= \int_{\Omega} f \bar{\psi}. \end{cases}$$

354 Substraction leads to

$$355 \quad a_0(\varphi_M - \varphi_0, \psi) = -d_M(\varphi_M, \psi).$$

356 Therefore we get

$$357 \quad |a_0(\varphi_M - \varphi_0, \psi)| \leq$$

$$358 \quad \left[M (Ms_0^2 + 2|k_\varepsilon|s_0) + \sqrt{2} \frac{Ms_1}{\varepsilon} \left(1 + \frac{Ms_1}{\varepsilon} \right) \right] \|\nabla \varphi_M\|_{L^2(\Omega)^2} \|\psi\|_{H^1(\Omega)},$$

359 which can be written, using $M < 1$:

$$360 \quad |a_0(\varphi_M - \varphi_0, \psi)| \leq MC_0 \|\nabla \varphi_M\|_{L^2(\Omega)^2} \|\psi\|_{H^1(\Omega)},$$

361 where C_0 is defined in (29). Taking $\psi = \varphi_M - \varphi_0$ leads to (30) and therefore to:

$$362 \quad \|\varphi_M - \varphi_0\|_{H^1(\Omega)} \leq \frac{MC_0}{C_0^c} \|\varphi_M\|_{H^1(\Omega)}.$$

363 We conclude using inequality Eq. (25). □

364 **5. The low Mach number approximation.** We look now for an approxima-
 365 tion $\tilde{\varphi}_M$ of the solution φ_M at low Mach numbers ($M \rightarrow 0$). In the previous section,
 366 we have shown that the no flow solution $\tilde{\varphi}_M = \varphi_0$ is not a good approximation of
 367 φ_M since the error was of order M . We will prove that $\tilde{\varphi}_M$, derived by neglecting
 368 the convection term $Mm\partial/\partial x$ in the convective operator $D_\varepsilon = Mm\partial/\partial x - ik_\varepsilon$, is a
 369 better approximation of φ_M . Indeed we will obtain that the error $\|\varphi_M - \tilde{\varphi}_M\|_{H^1(\Omega)}$
 370 is of order M^2 .

371 **5.1. Construction of the approximated model.** In this paragraph, we define
 372 the approximated Low Mach number model and we also introduce its solution $\tilde{\varphi}_M$.
 373 Moreover we prove that $\|\tilde{\varphi}_M - \varphi_0\|_{H^1(\Omega)} \sim M$ which results in $\|\varphi_M - \tilde{\varphi}_M\|_{H^1(\Omega)} \sim M^2$
 374 for M small.

375 **5.1.1. Approximation of the hydrodynamic unknown.** Let us recall that
 376 the hydrodynamic operator \mathbf{A}_M (see Eq. (14)) is defined for all φ in $H^1(\Omega)$ by :

$$377 \quad (31) \quad \begin{cases} A_M^{x,1} \varphi &= -\frac{m'(y)}{m(y)} \int_{-\infty}^x e^{i \frac{k_\varepsilon}{Mm(y)}(x-s)} \frac{\partial \varphi}{\partial y}(s, y) ds, \\ A_M^y \varphi &= \frac{m'(y)}{m(y)} \int_{-\infty}^x e^{i \frac{k_\varepsilon}{Mm(y)}(x-s)} \frac{\partial \varphi}{\partial x}(s, y) ds. \end{cases}$$

378 When $M = 0$, the integrals defining $\mathbf{A}_M \varphi$ in (31) are not defined. Moreover when
 379 $M \rightarrow 0$, these integrals are difficult to determine numerically: we have to evaluate

380 singular terms, highly oscillating integrals ($k_\varepsilon/M \rightarrow \infty$). We propose here an approx-
 381 imated formula to replace $\mathbf{A}_M \varphi$ when M is small. We introduce the following Low
 382 Mach number approximation, noted $\tilde{\mathbf{A}}_M \varphi$, defined for all φ in $H^1(\Omega)$ by:

$$383 \quad \tilde{\mathbf{A}}_M \varphi = (\tilde{A}_M^{x,1} \varphi, \tilde{A}_M^y \varphi)^T,$$

$$384 \quad = \left[-\frac{iMm'(y)}{k_\varepsilon} \frac{\partial \varphi}{\partial y}, \frac{iMm'(y)}{k_\varepsilon} \frac{\partial \varphi}{\partial x} \right]^T.$$

385 To get these expressions, we start from the exact expressions (31) and we suppose
 386 that φ is in $H^2(\Omega)$ (latter (32) will be applied to φ_0 which has the good regularity
 387 thanks to lemma 4) and we get after integration by parts:

$$388 \quad (32) \quad \begin{aligned} A_M^{x,1} \varphi &= -\frac{iMm'(y)}{k_\varepsilon} \left(\frac{\partial \varphi}{\partial y} - \int_{-\infty}^x e^{i\frac{k_\varepsilon}{Mm(y)}(x-s)} \frac{\partial^2 \varphi}{\partial x \partial y}(s, y) ds \right), \\ A_M^y \varphi &= \frac{iMm'(y)}{k_\varepsilon} \left(\frac{\partial \varphi}{\partial x} - \int_{-\infty}^x e^{i\frac{k_\varepsilon}{Mm(y)}(x-s)} \frac{\partial^2 \varphi}{\partial x^2}(s, y) ds \right). \end{aligned}$$

389 The Low Mach number approximation consists in keeping the first term in the above
 390 developments by supposing that the integral terms are negligible (we will show later
 391 that it is the case for $\varphi = \varphi_0$). The term $A_M^{x,2} \varphi$, corresponding to $A_\varepsilon^{x,2}$ in Eq. (14), is
 392 not taken into account because it is very small, of order M^2 , as shown in (36). The
 393 variational formulation associated to the Low Mach number approximation reads

$$394 \quad (33) \quad \begin{cases} \text{Find } \varphi \in H^1(\Omega) \text{ such that } \forall \psi \in H^1(\Omega), \\ \tilde{a}_M(\varphi, \psi) = \int_{\Omega} f \bar{\psi}. \end{cases}$$

395 $\tilde{a}_M(\varphi, \psi) = a_0(\varphi, \psi) + b_M(\varphi, \psi) + \tilde{c}_M(\varphi, \psi)$ with a_0 and b_M defined in (22) and (23).
 396 Moreover,

$$397 \quad (34) \quad \tilde{c}_M(\varphi, \psi) = \int_{\Omega} (\tilde{\mathbf{A}}_M \varphi) \cdot \nabla \bar{\psi},$$

398 and (33) is (21) with $c_M(\varphi, \psi)$ replaced by $\tilde{c}_M(\varphi, \psi)$. Note that we could also replace
 399 b_M by \tilde{b}_M , defined as b_M with the term weighted by M^2 cancelled. It would give
 400 the same quality of approximation $\|\varphi_M - \tilde{\varphi}_M\|_{H^1(\Omega)} \sim M^2$. However, as said in the
 401 introduction, only the term $\mathbf{A}_M \varphi$ is complicated to evaluate numerically and is worth
 402 being approximated at low Mach numbers.

403 **REMARK 5.** *As it is the case for $A_M^y \varphi$ and $A_M^{x,1} \varphi$ (see Eq. (15)), the terms $\tilde{A}_M^y \varphi$
 404 and $\tilde{A}_M^{x,1} \varphi$ are of order 1 in M in the sense that*

$$405 \quad (35) \quad \begin{cases} \left\| \tilde{A}_M^y \varphi \right\|_{L^2(\Omega)} \leq \frac{Ms_1}{|k_\varepsilon|} \left\| \frac{\partial \varphi}{\partial x} \right\|_{L^2(\Omega)}, \\ \left\| \tilde{A}_M^{x,1} \varphi \right\|_{L^2(\Omega)} \leq \frac{Ms_1}{|k_\varepsilon|} \left\| \frac{\partial \varphi}{\partial y} \right\|_{L^2(\Omega)}. \end{cases}$$

406 *These upper bounds are the same than the one obtained for A^M Eq. (27), replacing ε
 407 by k_ε . On the contrary, $A_M^{x,2}$ is of order 2:*

$$408 \quad (36) \quad \left\| A_M^{x,2} \varphi \right\|_{L^2(\Omega)} \leq \frac{M^2 s_1^2}{\varepsilon^2} \left\| \frac{\partial \varphi}{\partial x} \right\|_{L^2(\Omega)}.$$

409 *This is why a low Mach number approximation $\tilde{A}_M^{x,2}$ is not introduced for $A_M^{x,2}$.*

410 Before showing that $\tilde{\varphi}_M$ is an order 2 approximation of φ_M , let us prove that $\tilde{\varphi}_M$
411 exists.

412 **5.1.2. Well-posedness of the approximated model.** For M small enough,
413 the problem (33) is well-posed. Indeed, from (35) we get

$$414 \quad \left\| \tilde{A}_M \varphi \right\|_{L^2(\Omega)^2} \leq \frac{Ms_1}{|k_\varepsilon|} \|\nabla \varphi\|_{L^2(\Omega)^2},$$

415 from which we deduce that \tilde{a}_M is coercive for M small enough with the coercivity
416 constant:

$$417 \quad \tilde{C}_M^c = \min \left(\left[\frac{\varepsilon}{|k_\varepsilon|} (1 - M^2 s_0^2) - \frac{Ms_1}{|k_\varepsilon|} \right], \varepsilon |k_\varepsilon| \right).$$

418 Of course \tilde{C}_M^c is similar to (26).

419 **5.1.3. Quality of the low Mach number approximation.** Proceeding as in
420 Theorem 5, we can prove the estimation

$$421 \quad (37) \quad \|\tilde{\varphi}_M - \varphi_0\|_{H^1(\Omega)} \leq M \frac{\tilde{C}_0}{\tilde{C}_0^c \tilde{C}_M^c} \|f\|_{L^2(\Omega)},$$

422 where

$$423 \quad \tilde{C}_0 = s_0^2 + 2|k_\varepsilon|s_0 + \frac{s_1}{|k_\varepsilon|},$$

424 similarly to the constant (29). Now we will prove our main result: $\tilde{\varphi}_M$ is a good
425 approximation of φ_M in the sense that the error is bounded by M^2 :

426 **THEOREM 6.** *Let φ_M and $\tilde{\varphi}_M$ be the solution of (21) and (33). Then there exists*
427 *$C(M) > 0$ such that*

$$428 \quad \|\varphi_M - \tilde{\varphi}_M\|_{H^1(\Omega)} \leq C(M)M^2,$$

429 *with $C(M)$ bounded (C tends to a constant when $M \rightarrow 0$).*

430 *Proof.* If we denote

$$431 \quad (38) \quad e_M(\varphi, \psi) = a_0(\varphi, \psi) + b_M(\varphi, \psi),$$

432 Then using (21) and (33) we get

$$433 \quad e_M(\tilde{\varphi}_M - \varphi_M, \psi) = c_M(\varphi_M, \psi) - \tilde{c}_M(\tilde{\varphi}_M, \psi),$$

434 where c_M, \tilde{c}_M are defined in (24) and (34). The right hand side of the previous term
435 is more explicitly:

$$436 \quad c_M(\varphi_M, \psi) - \tilde{c}_M(\tilde{\varphi}_M, \psi) = \int_{\Omega} \left(A_M^{x,1} \varphi_M - \tilde{A}_M^{x,1} \tilde{\varphi}_M \right) \frac{\partial \bar{\psi}}{\partial x} + \left(A_M^{x,2} \varphi_M \right) \frac{\partial \bar{\psi}}{\partial x} + \left(A_M^y \varphi_M - \tilde{A}_M^y \tilde{\varphi}_M \right) \frac{\partial \bar{\psi}}{\partial y}. \blacksquare$$

437 We need to find an upper bound of this term: we write

$$438 \quad |c_M(\varphi_M, \psi) - \tilde{c}_M(\tilde{\varphi}_M, \psi)| \leq$$

$$439 \quad \left(\left\| A_M^{x,1} \varphi_M - \tilde{A}_M^{x,1} \tilde{\varphi}_M \right\|_{L^2(\Omega)} + \left\| A_M^{x,2} \varphi_M \right\|_{L^2(\Omega)} + \left\| A_M^y \varphi_M - \tilde{A}_M^y \tilde{\varphi}_M \right\|_{L^2(\Omega)} \right) \|\nabla \bar{\psi}\|_{L^2(\Omega)}, \blacksquare$$

440 and we will prove that each of the three terms in the right hand side is bounded by
441 M^2 .

- 442 • Terms $\left\|A_M^{x,1}\varphi_M - \tilde{A}_M^{x,1}\tilde{\varphi}_M\right\|_{L^2(\Omega)}$ and $\left\|A_M^y\varphi_M - \tilde{A}_M^y\tilde{\varphi}_M\right\|_{L^2(\Omega)}$
 443 Both terms can be treated in the same way and we just present the derivation
 444 of an upper bound for $A_M^{x,1}$. We use φ_0 as an intermediate field between φ_M
 445 and $\tilde{\varphi}_M$ and we write:

$$446 \left\|A_M^{x,1}\varphi_M - \tilde{A}_M^{x,1}\tilde{\varphi}_M\right\|_{L^2(\Omega)} = \left\|A_M^{x,1}(\varphi_M - \varphi_0) - \tilde{A}_M^{x,1}(\tilde{\varphi}_M - \varphi_0) + (A_M^{x,1} - \tilde{A}_M^{x,1})\varphi_0\right\|_{L^2(\Omega)},$$

$$447 \leq \left\|A_M^{x,1}(\varphi_M - \varphi_0)\right\|_{L^2(\Omega)} + \left\|\tilde{A}_M^{x,1}(\tilde{\varphi}_M - \varphi_0)\right\|_{L^2(\Omega)} + \left\|(A_M^{x,1} - \tilde{A}_M^{x,1})\varphi_0\right\|_{L^2(\Omega)}.$$

448 The reason of the introduction of φ_0 is that the $H^2(\Omega)$ regularity of φ_0 will
 449 be required to get estimates on $(A_M^{x,1} - \tilde{A}_M^{x,1})\varphi_0$ since Eq. (32) will be used.
 450 Here also three terms must be bounded. For the first two ones we have, using
 451 Theorem 5, inequalities (35) and (27), or more precisely

$$452 \left\|A_M^{x,1}\varphi\right\|_{L^2(\Omega)} \leq \frac{Ms_1}{\varepsilon} \left\|\frac{\partial\varphi}{\partial y}\right\|_{L^2(\Omega)},$$

453 and Eq. (37):

$$454 \left\|A_M^{x,1}(\varphi_M - \varphi_0)\right\|_{L^2(\Omega)} + \left\|\tilde{A}_M^{x,1}(\tilde{\varphi}_M - \varphi_0)\right\|_{L^2(\Omega)}$$

$$455 \leq Ms_1 \left(\frac{1}{|\varepsilon|} \|\varphi_M - \varphi_0\|_{H^1(\Omega)} + \frac{1}{|k_\varepsilon|} \|\tilde{\varphi}_M - \varphi_0\|_{H^1(\Omega)} \right) \leq C^\circ M^2,$$

456 where

$$457 C^\circ = s_1 \left(\frac{1}{|\varepsilon|} \frac{C_0}{C_0^c C_M^c} + \frac{1}{|k_\varepsilon|} \frac{\tilde{C}_0}{\tilde{C}_0^c \tilde{C}_M^c} \right) \|f\|_{L^2(\Omega)}.$$

458 For the last term, we use (32)

$$459 \left(A_M^{x,1} - \tilde{A}_M^{x,1} \right) \varphi_0 = M \frac{im'(y)}{k_\varepsilon} \int_{-\infty}^x e^{i \frac{k_\varepsilon}{Mm(y)}(x-s)} \frac{\partial^2 \varphi_0}{\partial x \partial y}(s, y) ds$$

$$460 = G_\varepsilon * M^2 \frac{im'(y)m(y)}{k_\varepsilon} \frac{\partial^2 \varphi_0}{\partial x \partial y}.$$

462 Note that this term is defined since $\varphi_0 \in H^2(\Omega)$, from lemma (4). We deduce
 463 the upper bound:

$$464 \left\| \left(A_M^{x,1} - \tilde{A}_M^{x,1} \right) \varphi_0 \right\|_{L^2(\Omega)} \leq C_{xy} M^2,$$

465 where

$$466 C_{xy} = \frac{s_1 s_0}{\varepsilon |k_\varepsilon|} \left\| \frac{\partial^2 \varphi_0}{\partial x \partial y} \right\|_{L^2(\Omega)}.$$

467 Collecting all the terms together, we obtain

$$468 \left\| A_M^{x,1}\varphi_M - \tilde{A}_M^{x,1}\tilde{\varphi}_M \right\|_{L^2(\Omega)} \leq (C^\circ + C_{xy}) M^2.$$

469 In a same way we get

$$\|A_M^y \varphi_M - \tilde{A}_M^y \tilde{\varphi}_M\|_{L^2(\Omega)} \leq (C^\circ + C_{xx})M^2.$$

with

$$C_{xx} = \frac{s_1 s_0}{\varepsilon |k_\varepsilon|} \left\| \frac{\partial^2 \varphi_0}{\partial x^2} \right\|_{L^2(\Omega)}.$$

• Term $\|A_M^{x,2} \varphi_M\|_{L^2(\Omega)}$

From Eq. (36) and (25) is deduced:

$$\|A_M^{x,2} \varphi_M\|_{L^2(\Omega)} \leq \frac{M^2 s_1^2}{\varepsilon^2} \|\varphi_M\|_{H^1(\Omega)} \leq M^2 C^\bullet,$$

where

$$C^\bullet = \frac{s_1^2 \|f\|_{L^2(\Omega)}}{\varepsilon^2 C_M^c}.$$

Combining all the results together, we get the global estimation:

$$|e_M(\varphi_M - \tilde{\varphi}_M, \psi)| = |c_M(\varphi_M, \psi) - \tilde{c}_M(\tilde{\varphi}_M, \psi)| \leq M^2 [2C^\circ + C_{xy} + C_{xx} + C^\bullet] \|\nabla \psi\|_{L^2(\Omega)}^2,$$

from which we deduce, taking $\psi = \varphi_M - \tilde{\varphi}_M$:

$$\|\varphi_M - \tilde{\varphi}_M\|_{H^1(\Omega)} \leq \frac{[2C^\circ + C_{xy} + C_{xx} + C^\bullet]}{C_e^c} M^2,$$

with the coercivity constant for $e_M(\varphi, \psi)$:

$$C_e^c = \min \left(\frac{\varepsilon}{|k_\varepsilon|} (1 - M^2 s_0^2), \varepsilon |k_\varepsilon| \right) > 0. \quad \square$$

Finally, using Eq. (26), C° and C^\bullet depend on M but become constant when $M \rightarrow 0$ (see also remark 4).

6. Numerical validation.

6.1. Numerical setup. To solve numerically the Goldstein equations, we do not use the dissipative model. On the contrary we take $\varepsilon = 0$ and we introduce Perfectly Matched Layers (PMLs) to bound the calculation domain while selecting the outgoing solution. The advantage of using PMLs is that the solution in the neighborhood of the source f (more precisely outside the PMLs) is the physical one, since the unmodified Goldstein equations are solved there. The Goldstein equations in the PMLs are simply obtained by replacing $\partial/\partial x$ by $\alpha \partial/\partial x$. The complex number α is the PML parameter [41, 28] and has to be chosen such that $\Re(\alpha) > 0$ and $\Im(\alpha) < 0$ to select properly the outgoing solution.

In a guide of height h , the computational domain Ω_c , represented in Fig. 2, is defined as $\Omega_c = \Omega_b \cup \Omega_\pm^L$ where $\Omega_b = (0, d) \times (0, h)$ is a bounded domain around the source f and Ω_\pm^L are the PMLs of length L . We take the source $f(x, y) = 1$ in the disc of center $(d/2, h/2)$ and of radius $h/4$. The Goldstein equations are solved with the Finite Element code Xlife++ [42] at the frequency $k = 2$, for a unitary guide $h = 1$ and for PMLs such that $L = 0.5$ and $\alpha = (1 - i)/10$. Eq. (12) can be solved with classical Finite Element but not the hydrodynamic equation of (11). We could use Discontinuous Galerkin elements but for simplicity we preferred to use a Streamline Upwind Petrov-Galerkin (SUPG) formulation [43] of (11), introducing an extra parameter to the PML parameter α but allowing to use Continuous Finite Elements.

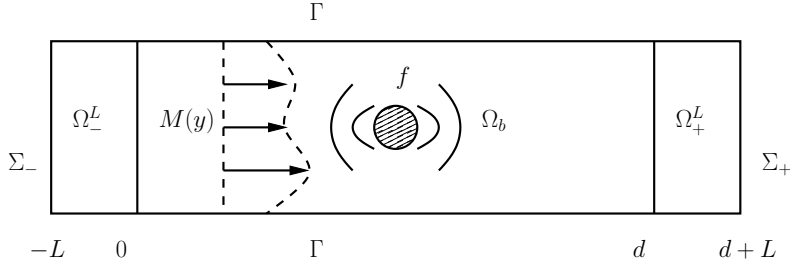


FIG. 2. Computation domain with the PMLs

507 **6.2. Numerical results.** We have considered three velocity profiles $m(y)$ de-
 508 fined in Eq. (20): a polynomial profile $m(y) = [0.25 + y + 10y(y - 0.5)(y - 1)]/1.25$,
 509 a sine profile $m(y) = [1.5 + \sin(2\pi y)]/2.5$ and a hyperbolic tangent profile $m(y) =$
 510 $[0.5 + 1 + \tanh(10(y - 0.5))]/2.5$. These profiles are drawn in Fig. 3 (a), Fig. 4 (a)
 511 and Fig. 5 (a). The profiles have been chosen such that $m(y) \in [0.2, 1]$. We note φ
 512 the exact solution and φ_{LM} the Low Mach number approximation. For $d = 1$, the
 513 relative H^1 errors $\|\varphi - \varphi_{LM}\|_{H^1(\Omega_b)} / \|\varphi\|_{H^1(\Omega_b)}$ versus M are plotted in red in Fig. 3
 514 (b), Fig. 4 (b) and Fig. 5 (b) for the three velocity profiles. The fits of the curves,
 515 represented in blue dashed lines, show that the H^1 errors is of the form $C_1 M^p$ with
 516 $p = 2.14$ for the polynomial profile, $p = 2.23$ for the sine profile and $p = 2.33$ for the
 517 hyperbolic tangent profile. The powers are very close to 2, predicted theoretically.
 518 We have tested other velocity profiles, linear combinations of cosine functions (results
 519 not reported here) and powers close to 2 have always been found. For the polynomial
 520 profile, the relative H^1 error is found very good for $M < 0.1$, below 1% and becomes
 521 bad for $M \sim 0.3$, where it reaches 10% (it reaches 10% for $M \sim 0.25$ for the sine
 522 profile and for $M \sim 0.20$ for the tangent profile). Note that the H^1 error is rather
 523 demanding, the relative error with the L^2 -norm is better. The L^2 -error reaches 10%
 524 for larger values of the Mach Number than with the H^1 -norm: for $M \sim 0.45$ for
 525 the polynomial profile, for $M \sim 0.40$ for the sine profile and for $M \sim 0.35$ for the
 526 tangent profile. The L^2 -error is again like $C_2 M^p$ with $p = 2.03$ for the polynomial
 527 profile, $p = 2.14$ for the sine profile and $p = 2.25$ for the hyperbolic tangent profile.
 528 The values of p are very close between the L^2 -norm and H^1 -norm: it means that the
 529 better results obtained with the L^2 -norm are due to a better constant: $C_2 < C_1$.

530 The dependence of the constant C_1 versus the parameters of the problem, al-
 531 though explicit (see proof of theorem 6), is not easy to analyze since all the param-
 532 eters are mixed together. But from the numerical tests, general tendencies can be
 533 extracted: the results are less good (C_1 increases) when k , s_0 (the maximum of the
 534 velocity) or s_1 (the maximum of the shear) increase. In particular the shear s_1 is
 535 important: indeed for $s_1 = 0$, since it implies that $M'(y) = 0$, then $\xi = \mathbf{0}$ for the
 536 exact solution and the Low Mach number approximation becomes exact. It is why the
 537 results are better for the polynomial profile and the worst for the hyperbolic tangent
 538 profile, this latter profile corresponding to the strongest $M'(y)$ values in the numerical
 539 tests.

540 To understand why the Low Mach number approximation gives so good results, it
 541 is useful to look at the fields. We present them for the polynomial profile, for $M = 0.1$
 542 and $M = 0.5$ and for a larger domain $d = 2$.

543 For a slow flow $M = 0.1$, in Fig. 6 are represented, only in Ω_b (outside the PMLs),

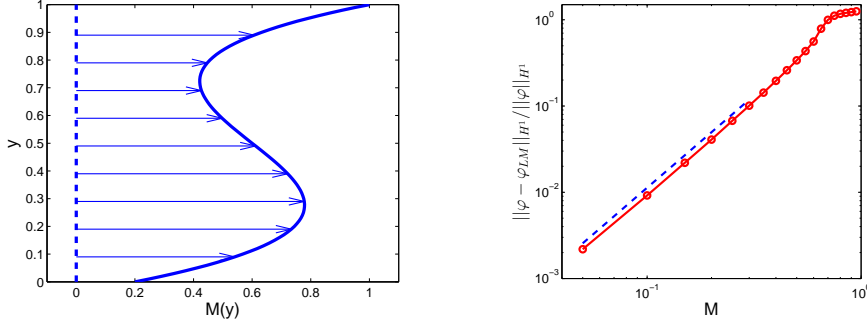


FIG. 3. (a): polynomial velocity profile; (b): H^1 errors versus M in red, fit in blue

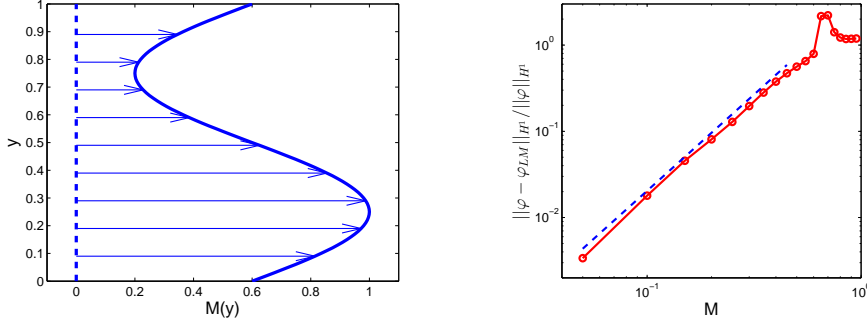


FIG. 4. (a): sine velocity profile; (b): H^1 errors versus M in red, fit in blue

544 $\Re(\varphi)$ and $\Re(\varphi_{LM})$: as expected, they are very similar. In complement, Fig. 7 shows
 545 $\Im(\xi_x)$ and $\Im(\xi_{LM}^x)$ and Fig. 8 shows $\Im(\xi_y)$ and $\Im(\xi_{LM}^y)$. For both components
 546 of ξ , we see that the Low Mach number approximation captures satisfactorily the long
 547 wavelength phenomena and neglects the fast oscillatory phenomena. ξ and ξ_{LM} seem
 548 rather different but let us recall that the error on ξ is expected to be stronger than
 549 the error on φ : it varies only like M whereas it varies like M^2 for φ .

550 For a faster flow $M = 0.5$, Fig. 9 shows $\Re(\varphi)$ and $\Re(\varphi_{LM})$: we see that φ_{LM}
 551 approximates badly φ , the Low Mach number approximation being unable to capture
 552 the hydrodynamic phenomena, associated to short wavelengths. However the long
 553 wavelength phenomena in φ are rather well recovered in φ_{LM} . This is surprising
 554 for this rather large M value and also because ξ and ξ_{LM} are found very different
 555 (comparison not shown here).

556 **7. Conclusion.** To study the time-harmonic acoustic propagation in a general
 557 flow, starting from the exact Goldstein equations we have developed a new model,
 558 the Low Mach number Approximation of the Goldstein equations (4)-(5), which has
 559 two main features: it is much simpler than the initial Goldstein equations because the
 560 transport operator solving Eq. (5) is replaced by the explicit relation (9). Moreover it
 561 is able to take into account the convection of vortices, contrary to the usual convected
 562 Helmholtz equation (1) which restricts to acoustics phenomena. For a parallel shear
 563 flow, we have proved theoretically and confirmed numerically that this approximated
 564 model is very accurate, in the sense that the error on the acoustic field is of order

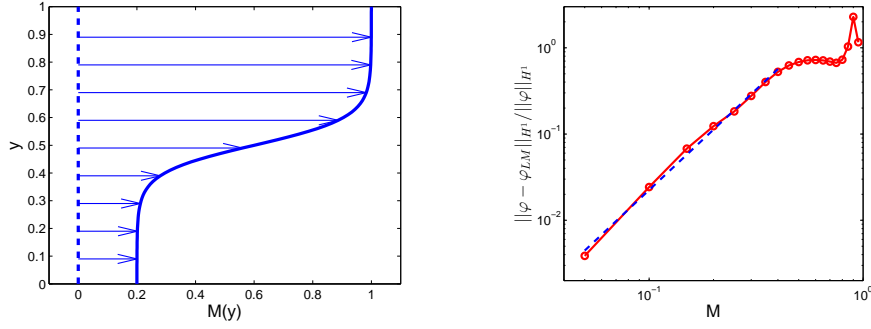


FIG. 5. (a): hyperbolic tangent velocity profile; (b): H^1 errors versus M in red, fit in blue

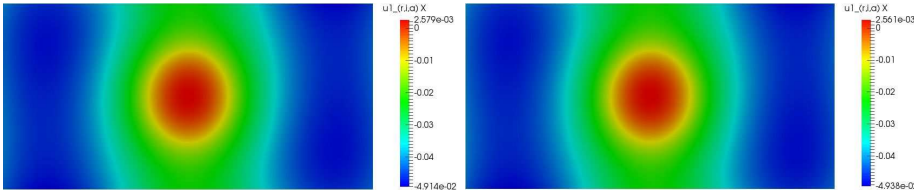


FIG. 6. $\Re(\varphi)$ and $\Re(\varphi_{LM})$ in Ω_b for a polynomial velocity profile and $M = 0.1$

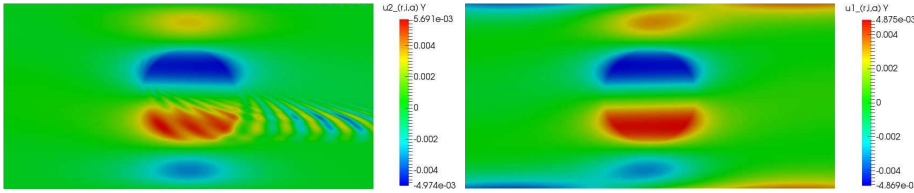


FIG. 7. $\Im(\xi_x)$ and $\Im(\xi_{LM}^x)$ in Ω_b for a polynomial velocity profile and $M = 0.1$

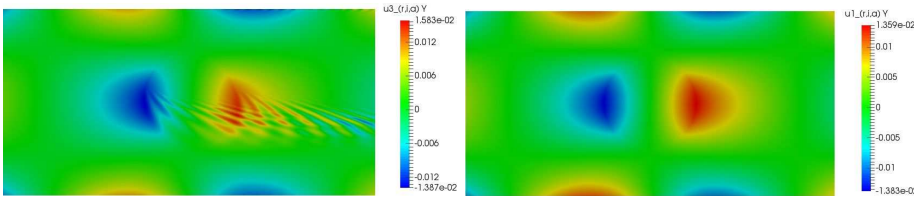


FIG. 8. $\Im(\xi_y)$ and $\Im(\xi_{LM}^y)$ in Ω_b for a polynomial velocity profile and $M = 0.1$

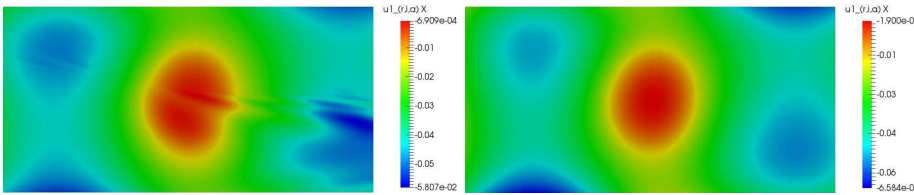


FIG. 9. $\Re(\varphi)$ and $\Re(\varphi_{LM})$ in Ω_b for a polynomial velocity profile and $M = 0.5$

565 two, bounded by the square of the Mach number.

566 The generalization of this result to a non-parallel 2D or 3D flow is not straight-
 567 forward and would be very technical: indeed it would require to perform a change of
 568 variables to transform the transport equation (5) in a family of ordinary differential
 569 equations along the streamlines of the carrier flow. But we think that the accuracy
 570 of the Low Mach number model (10), rigorously proved for a shear flow, remains
 571 valid for any flow. This general Low Mach number model (10) is much simpler than
 572 the initial one (4)-(5), which is particularly interesting for 3D applications, and is
 573 certainly much better than Eq. (1): extrapolating the results obtained for a parallel
 574 shear flow, the acoustic error should be of order M^2 (instead of M for Eq. (1)) where
 575 M is the characteristic Mach number of the carrier flow. Moreover this Low Mach
 576 number model has good mathematical properties, contrary to the general model: for
 577 instance it is easy to prove that it is well-posed as soon as $\exists \beta > 0$ such that

$$578 \quad \inf_{\mathbf{x} \in \Omega} \left[1 - \left(\frac{\mathbf{v}_0}{c_0} \right)^2 - \frac{|\boldsymbol{\omega}_0|}{\omega} \right] \geq \beta,$$

579 and it is of course naturally the case for a slow flow.

580

REFERENCES

- 581 [1] S. Mancini, R. J. Astley, S. Sinayoko, G. Gabard and M. A. Tournour, Variable transformation
 582 approach for boundary element solutions of wave propagation in non-uniform potential flows,
 583 Inter-Noise, Hamburg (2016).
- 584 [2] N. Balin, F. Casenave, F. Dubois, E. Duceau, S. Duprey and I. Terrasse, Boundary element and
 585 finite element coupling for aeroacoustics simulations, *Journal of Computational Physics* **294**,
 586 274-296 (2015).
- 587 [3] P. Destuynder and E. Gout-D'hénin, Sur l'existence et l'unicité de solutions de modèles linéaires
 588 en aéroacoustique, *Comptes Rendus de l'Académie des Sciences-Series I-Mathematics*
 589 **332**(2), 183-188 (2001).
- 590 [4] W. Eversman, The Boundary condition at an Impedance Wall in a Non-Uniform Duct with
 591 Potential Mean Flow, *J. Acoust. Soc. Am.* **246**(1), 63-69 (2001).
- 592 [5] D. Blokhintzev, The propagation of sound in an inhomogeneous and moving medium I., *J. Acoust.*
 593 *Soc. Am.* **18**(2), 322-328 (1946).
- 594 [6] A. D. Pierce, Wave equation for sound in fluids with unsteady inhomogeneous flow, *J. Acoust.*
 595 *Soc. Am.* **87**(6), 2292-2299 (1990).
- 596 [7] D. C. Pridmore Brown, Sound propagation in a fluid flowing through an attenuating duct, *The*
 597 *Journal of the Acoustical Society of America* **30**(7), 670-670 (1958).
- 598 [8] M. Oppeneer, S. W. Rienstra and P. Sijtsma, P., *Efficient Mode Matching Based on Closed-Form*
 599 *Integrals of Pridmore-Brown Modes*, *AIAA Journal* **54**(1), 266-279 (2015).
- 600 [9] E. J. Brambley, M. Darau and S. W. Rienstra, The critical layer in linear-shear boundary layers
 601 over acoustic linings, *J. Fluid Mech.* **710**, 545568 (2012).
- 602 [10] A. Agarwal, P. J. Morris and R. Mani, Calculation of sound propagation in nonuniform flows:
 603 suppression of instability waves, *AIAA journal* **42**(1), 80-88 (2004).
- 604 [11] E. J. Brambley and G. Gabard, Reflection of an acoustic line source by an impedance surface
 605 with uniform flow, *Journal of Sound and Vibration* **333**(21), 5548-5565 (2014).
- 606 [12] D. Dagna and P. Blanc-Benon, Sound radiation by a moving line source above an impedance
 607 plane with frequency-dependent properties, *Journal of Sound and Vibration* **349**, 259-275
 608 (2015).
- 609 [13] M. Myers, On the acoustic boundary condition in the presence of flow, *J. Acoust. Soc. Am.*
 610 **71**(3), 429-434 (1980).
- 611 [14] E. J. Brambley, Well-posed boundary condition for acoustic liners in straight ducts with flow,
 612 *AIAA Journal* **49**(6), 1272-1282 (2011).
- 613 [15] G. Gabard, A comparison of impedance boundary conditions for flow acoustics, *Journal of*
 614 *Sound and Vibration* **332**(4), 714-724, (2013).
- 615 [16] H. Galbrun, Propagation d'une onde sonore dans l'atmosphère terrestre et théorie des zones de
 616 silence, Gauthier-Villars, Paris, France (1931).

- 617 [17] F. Treyssede, G. Gabard, and M. B. Tahar, A mixed finite element method for acoustic wave
618 propagation in moving fluids based on an Eulerian-Lagrangian description, *J. Acoust. Soc.*
619 *Am.* **113**, 705-716 (2003).
- 620 [18] A. S. Bonnet-Ben Dhia, J. F. Mercier, F. Millot, S. Pernet and E. Peynaud, Time-Harmonic
621 Acoustic Scattering in a Complex Flow: A Full Coupling Between Acoustics and Hydrody-
622 namics, *Commun. Comput. Phys.* **11**(2), 555-572 (2012).
- 623 [19] W. A. Möhring, A well proposed acoustic analogy based on a moving acoustic medium, *Proceed-*
624 *ings 1st Aeroacoustic Workshop (in connection with the german research project SWING)*,
625 Dresden (1999).
- 626 [20] C. Legendre, G. Lielens, J.-P. Coyette, Sound Propagation in a sheared flow based on fluctuating
627 total enthalpy as generalized acoustic variable, *Proceedings of of the Internoise 2012/ASME*
628 *NCAD meeting*, New York City, NY, USA (2012).
- 629 [21] M. E. Goldstein, Unsteady vortical and entropic distortion of potential flows round arbitrary
630 obstacles, *J. Fluid Mech.* **89**(3), 433-468 (1978).
- 631 [22] S. E. P. Bergliaffa, K. Hibberd, M. Stone and M. Visser, Wave Equation for Sound in Fluids
632 with Vorticity, *Physica D* **191**, 121-136 (2004).
- 633 [23] A. J. Cooper, Effect of mean entropy on unsteady disturbance propagation in a slowly varying
634 duct with mean swirling flow, *J. Sound Vib.* **291**(3-5), 779-801 (2006).
- 635 [24] C. J. Heaton and N. Peake, Algebraic and exponential instability of inviscid swirling flow, *J.*
636 *Fluid Mech.* **565**, 279-318 (2006).
- 637 [25] M. R. Myers and E. J. Kerschen, Influence of camber on sound generation by airfoils interacting
638 with high-frequency gusts, *Journal of Fluid Mechanics* **353**, 221-259 (1997).
- 639 [26] M. E. Goldstein, M. Z. Afsar and S. J. Leib, Non-homogeneous rapid distortion theory on
640 transversely sheared mean flows, *Journal of Fluid Mechanics* **736**, 532-569 (2013).
- 641 [27] L. J. Ayton and N. Peake, On high-frequency sound generated by gust-aerofoil interaction in
642 shear flow, *Journal of Fluid Mechanics* **766**, 297-325 (2015).
- 643 [28] E. Bécache, A.-S. Bonnet-Ben Dhia, and G. Legendre, Perfectly matched layers for time-
644 harmonic acoustics in the presence of a uniform flow, *SIAM J. Numer. Anal.* **44**, 1191-1217
645 (2006).
- 646 [29] F. Nataf, A new approach to perfectly matched layers for the linearized Euler system, *J. Comput.*
647 *Phys.* **214**, 757-772 (2006).
- 648 [30] F. Q. Hu, A perfectly matched layer absorbing boundary condition for linearized Euler equations
649 with a non-uniform mean flow, *Journal of Computational Physics* **208**(2), 469-492 (2005).
- 650 [31] G. Gabard, Discontinuous Galerkin methods with plane waves for time-harmonic problems,
651 *Journal of Computational Physics* **225**, 1961-1984 (2007).
- 652 [32] A. Ern and J.-L. Guermond, Theory and practice of finite Element, *Applied Mathematical*
653 *Sciences*, Springer-Verlag, New York (2004).
- 654 [33] K. Taylor, Acoustic generation by vibrating bodies in homentropic potential flow at low Mach
655 number, *Journal of Sound and Vibration* **65**(1), 125-136 (1979).
- 656 [34] C. Clancy and H. J. Rice, Acoustic shielding in low Mach number potential flow incorporating
657 a wake model using bem. In 15th AIAA/CEAS Aeroacoustics Conference (2009).
- 658 [35] V. Pagneux and B. Froelich, Influence of low Mach number shear flow on acoustic propagation
659 in ducts, *Journal of Sound and vibration* **246**(1), 137-155 (2001).
- 660 [36] A. S. Bonnet-Ben Dhia, J.-F. Mercier, F. Millot and S. Pernet, A low Mach model for time
661 harmonic acoustics in arbitrary flows, *J. of Comp. and App. Math.* **234**(6), 1868-1875 (2010).
- 662 [37] J. H. Seo and Y. J. Moon, Linearized perturbed compressible equations for low Mach number
663 aeroacoustics, *J. Comput. Phys.* **218**, 702-719 (2006).
- 664 [38] C. D. Munz, M. Dumbser and S. Roller, Linearized acoustic perturbation equations for low
665 Mach number flow with variable density and temperature, *Journal of Computational Physics*
666 **224**(1), 352-364 (2007).
- 667 [39] P. G. Drazin and W. H. Reid, Hydrodynamic stability, Cambridge university press (2004).
- 668 [40] H. Brézis. Analyse fonctionnelle, théorie et applications, Masson, Paris, France (1983).
- 669 [41] A. S. Bonnet-Ben Dhia, E. M. Duclairoir and J. F. Mercier, Acoustic propagation in a flow:
670 numerical simulation of the time-harmonic regime, *ESAIM Proceedings* **22** (2007).
- 671 [42] <http://uma.ensta-paristech.fr/soft/XLiFE++/>
- 672 [43] T. J. R. Hughes and A. Brooks, Streamline upwind/Petrov-Galerkin formulation for convection
673 dominated flows with particular emphasis on the incompressible Navier-Stokes equations,
674 *Comp. Meth. Appl. Mech. Engrg.* **32**, 199-259 (1982)